New Approach for Predicting Multiple Fractured Horizontal Wells Performance in Tight Reservoirs

Mojtaba MoradiDowlatabad, Mahmoud Jamiolahmady, Heriot-Watt University

Abstract

Multiple fractured horizontal wells (MFHWs) are considered as the most effective stimulation technique to improve recovery from low permeability reservoirs particularly tight and shale assets. Understanding of the complex flow behaviour and predicting Productivity Index (PI) of these wells are vital for exploitation of unconventional reservoirs.

The analytical or semi analytical models previously proposed for their PI calculations cannot accurately describe the flow behaviour around MFHWs mainly due to lack of capturing the complexity of the flow especially the fracture-to-fracture interference effects. Many of them are also too complex and/or not general enough limiting their use. The fine grid three-dimensional (3D) simulation approach is also costly and cumbersome. In this work, we followed a new approach to develop a new equation that can predict MFHWs performance under pseudo-steady state (PSS) flow conditions in tight reservoirs.

A programming code, producing the include files, was coupled with a fine grid 3D commercial reservoir simulator to generate a large data bank. For these simulations, the pertinent parameters (matrix permeability, the number of fractures and fracture permeability, spacing, width, length and conductivity) were varied over wide practical ranges based on the Latin Hypercube sampling method.

The individual impact of the parameters on PI, as the output variable, was evaluated by a statistical analysis technique under different prevailing conditions. It is shown, for instance, that increasing the fracture width and permeability does not result in a significant monotonic increase in PI while changing fracture length, spacing and numbers influence PI greatly.

A new equation is then proposed that relates MFHWs-PI to a limited number of parameters by applying symbolic regression technique. Here, the total productivity index of MFHWs is related to the PI of the horizontal well with a single fracture, the number of fractures and dimensionless fracture spacing. The cross-validation results show that the proposed equation is general, reliable and simple for prediction purposes because it benefits from limited and appropriate dimensionless numbers with good values of fitting indices.

This study expands our understanding of flow behaviour in tight reservoirs and provides an invaluable engineering tool that can facilitate simulation of flow around MFHWs, their optimum design and their well performance prediction.

1. Introduction

Conventionally, the permeability of a reservoir rock needs to be between 0.001 and 0.1 mD (9.87e-16 to 9.87e-14 m^2) to be classified it as a tight reservoir [20]. Compared to vertical wells, horizontal wells are more suitable for low-permeability, thin reservoirs. However, advantages of the horizontal wells diminish with a decrease in reservoir permeability especially vertical permeability. This situation can be improved by the staged fracturing technique to generate multiple fractured horizontal wells [23]. Understanding of the complex flow behaviour and predicting Productivity Index (PI) of these wells are vital for exploitation of unconventional reservoirs.

Current methods for productivity evaluation of MFHWs have their own drawbacks [1-4]. Giger [5] proposed semi-analytical models for steady state flow around a horizontal well with intersecting fractures. In this approach, flow within the fracture and from the matrix was assumed radial and the total flow rate was calculated through multiplying the flow rate of each fracture by the number of fractures. Guo and Evans [6] used a similar approach to that of Giger et al. and developed another formulation for predicting the well performance of a horizonal well intersecting a naturally fractured system but under pseudo-steady state (PSS) conditions. Mukherjee and Economides [7] combined Joshi [8] and Prats [9] works to develop a new model to predict productivity index (PI) at steady state conditions. Raghavan and Joshi [2] applied the principle of superposition to predict productivity of horizontal wells with multiple transverse fractures. This equation has several limitations, for example, the fracture spacing should be larger than the fracture half-length and the complexity (number) of the equations increases as the number of fracture increases. In another study, Guo and Schechter [10] developed an equation based on the reservoir linear flow and fracture linear flow. Wan and Aziz (2002) also developed a semi-analytical model for MFHWs by applying Fourier analysis to calculate PI at PSS conditions. Kuppe and Settari [11] presented an empirical equation for predicting the performance of the MFHWs in the conventional oil reservoirs. They used traditional, nonlinear regression to modify the equation proposed by Mukherjee and Economides [7].

A more practical formulation proposed by Guo, Zeng, Zhao and Xu [12] included the effect of fracture length, azimuth angle, conductivity, the number of fractures and symmetry of the fractures under pseudo-steady state conditions. Here, the total pressure drop was assumed to be a summation of series of individual pressure drop values corresponding to various flow regimes, which makes it complex and not general.

A number of researchers [13, 14] have used the distributed volumetric sources method to calculate the dimensionless productivity index of MFHWs under transient or pseudo-steady state conditions. In this complex, semi-analytical approach, they have included the pressure variation inside the fracture. The proposed solution consists of complex series of instantaneous Green's mathematical functions. With such methods, the fracture conductivity is either assumed infinite that leads to overestimating the productivity, or treated as finite in which the complicated equation must be solved with boundary integral methods. Some investigators used nonlinear regression to develop complex equations for predicting net present value or PI increment [15, 16] for MFHWs application. The problem with theses equations is that they are not descriptive enough to clearly show the relationship between the desired output and the input variables.

Therefore, it is recognised that the analytical or semi analytical models available in the literature cannot accurately describe the flow behaviour around MFHWs due to lack of capturing the complexity of the flow especially the fracture-to-fracture interference effects. Fig 1 shows the normalised production flow rates of each fracture of a MFHW case, which is shown in Fig 2, and has five fractures with same properties. It is noted that in this reservoir with formation permeability of 0.01 mD, although the fractures are uniform, the fracture flow rates are not equal due to the fracture interference and different drainage area. As estimating the drainage area for each fracture is impossible, the developed equations are believed to be more suitable for predicting the performance of the wells with a single fracture or for specific MFHWs configurations and not valid for most of the MFHWs applications in tight reservoirs. It should also be noted that the explicit numerical modelling of the MFHWs requires fine gridding that makes 3D simulation approach costly and cumbersome.

In this work, we followed a novel approach to develop a new empirical equation that can predict MFHWs performance under pseudo steady state conditions. The advanced mathematical technique (Symbolic regression) along with the statistical sampling method (Latin Hypercube) was used to deliver an equation for capturing the MFHW flow performance including the fracture interference.

This study aims to expand our understanding of flow behaviour in tight reservoirs and provides an invaluable engineering tool that can facilitate simulation of flow around MFHWs and prediction of the corresponding well performance. It also facilitates the optimum hydraulic fracture design and the long-term well performance prediction of such wells.

2. Numerical Simulation

The performance of MFHWs in tight reservoirs can be explained by series of very complex flow regimes developed during the production time. Assuming a perfect clean-up is performed [17], after passing the fracture linear flow regime, at the early times, linear flow from formation to each fracture will be developed corresponding to "formation linear flow regime". If constant finite conductivity within the fracture is assumed, this flow regime could be represented in the form of "bilinear flow regime". It is most likely that the expected "early formation radial flow regime" will not follow due to the fracture interference effect. Then fracture interference effect is felt, which leads to a "transitional flow regime" to a complete "compound linear flow regime". At this stage, the region between the fractures is depleted while the outer edge of the pressure transient gradually shifts its orientation such that the bulk flow is linear toward the set of fractures. Next, "pseudo elliptical flow" regime may be observed and finally as pressure profile reaches the boundary, "Pseudo steady state" or boundary dominated flow regime will be developed to represent the flow from farther reservoir. The time for the pressure to establish a boundary-dominated flow could be estimated by:

$$t_{pss} = 3790 \frac{\emptyset \mu C_t A}{K_m} t_{DApss} \qquad \text{Equation 1}$$

where t_{pss} is the PSS time and t_{DApss} is the shape factor value, which depends on the geometry and well placement. Considering the practical fracture spacing, fracture half-length and the diffusivity of the tight formation, some of the flow regimes before the PSS condition may not be recorded for all cases.

For the simulations conducted during this study, the pertinent parameters [matrix permeability (K_m), fracture permeability (K_f), fracture half-length (X_f), fracture width (W_f), number of fractures (N_f) and fracture spacing (S_f)] were varied over wide practical ranges based on the Latin Hypercube sampling method with input from our industrial sponsors. To generate the large data bank required to propose a general solution, a programming code, which automatically creates required include-files and stores relevant output data for each simulation, was coupled with a fine grid 3D reservoir model.

Some of the simulations results were used to train and finalise the equation, whereas some were used for testing predictive capabilities of the proposed equation. In this process, the impacts of important parameters were also studied individually initially and then combined to ensure an efficient general formulation is achieved.

2.1 Base Case Model Description

A 3D Cartesian grid model was constructed by a commercially available reservoir simulator to model a tight reservoir with MFHWs. A horizontal well with the maximum length of the reservoir half-length completed with up to 15 fractures placed in the centre of a box-shaped homogeneous reservoir model, (Fig 2). Due to much more complex flow behaviour around a MFHW compared to that around a conventional well, the local grid refinement, which explicitly defines hydraulic fractures in the simulation, is required to properly capture the changes in flow parameters, when the fluid travels from the matrix to the fractures and then to the wellbore, as performed here. The model contains 451*301*10 grid cells with a dimension of 20*20*10 ft in the X, Y and Z direction, respectively. The gridding was selected based on a sensitivity analysis on the global grid size to avoid numerical dispersion while keeping run time reasonable. In addition, another sensitivity analysis on the grid refinement was carried out to determine the optimum number of grids around each fracture. The optimum local grid refinement around each fracture used in this study divided each parent grid into 9 sub girds in the X, 4 sub grids in the Y and 1 grid in the Z directions.

The hypothetical tight reservoir has an area of 1246 acres producing with an initial reservoir pressure of 7,500 psi (5.17e+7 N/m^2). The fluid flow occurred within the reservoir with the average effective reservoir permeability (K_m), assumed to vary between 0.001 and 0.1 mD. The selected control mode was a 250 Mscf/day (0.08 SM^3/sec) production rate to ensure developing pseudo-steady state flow regime for all cases. Table 1 and Table 2 provide more information on the model's properties and investigated parameters. The following additional assumptions were also made:

1) The produced single-phase fluid was Newtonian and its flow within the fractures and the matrix was governed by Darcy law as a proper clean up prior to the well production was assumed.
2) The horizontal well was oriented in the direction of least in-situ horizontal stress of formation, resulting in the vertical planar fracture aligned in the y-direction after hydraulic fracturing.
3) For all simulations, the hydraulic fractures were identical, i.e. they were positioned vertically with constant spacing along the well and penetrated the whole reservoir thickness with same properties.
4) The well was completed with cemented liner assuming no pressure loss along the horizontal hole section. Considering MFHWs with the cased/perforated completion, the flow to the wellbore was only from hydraulic fractures introduced along the wellbore at the specific locations.
5) No geomechanics effects were considered in this study as it is expected that the impact not to be significant for the considered range of permeabilities. In other words, the formation and fracture properties do not change throughout a simulation.

The impacts of all pertinent parameters were considered in a pre-screening sensitivity exercise to identify the parameters affecting PI significantly from those with minimal effects. For instance, rock compressibility did not affect the PI values when it was changed within a range of 1E-7 to 3E-5 1/psi. in this study, the rock compressibility was fixed to be 3.82E-6 psi^{-1}. Table 2 provides the variation ranges of chosen pertinent parameters used for assessing the relative sensitivity of productivity index to individual parameters. As mentioned earlier, these were selected to cover reasonably wide practical ranges as suggested by our industrial partners.

3. Statistical Analysis of Effective Parameters

3.1 Latin Hypercube Sampling

Experimental design (Sampling) methods are widely used to efficiently sample among all the possibilities to identify the full impact of all pertinent parameters. Latin Hypercube Sampling, first introduced by McKay [18], is a statistical method for generating a sample of possible collections of parameter values from a multidimensional distribution randomly, but systematically. In this study, 2000 simulations with various MFHWs designs were generated by applying the Latin Hypercube sampling method to fully investigate the impact of these parameters. Distributions of the variables were assumed uniform as shown in Table 2. N_f, S_f and X_f were varied within the ranges of (1-15), (80-650 ft) and (100-1020 ft) while K_f and W_f were changed from 2 to 8 mm and from 10 to 200 mD, respectively. A pre-processor code in Python was programmed to generate 2000 MFHWs designs and produce the include files required for the reservoir simulation. It should be noted that the well length is not limited to a specific value allowing us to investigate the performance of installing a different number of fractures at various spacing.

When changing the parameters in the simulation model, the average reservoir pressure ($\bar{P}_r$) and its corresponding flowing bottom-hole pressure (P_{wf}), both in psi, at the PSS conditions were recorded for individual case to calculate the well productivity for slightly compressible fluid by the following equation:

$$PI = \frac{Q}{\bar{P}_r - P_{wf}} \quad \text{Equation 2}$$

where Q is the rate of production.

3.2 Spearman's Rank Correlation Coefficient

It is appropriate to compare the relationship between several input-output pairs of data using a statistical approach. Spearman's rank correlation coefficient (rho) is such a quantitative measure of dependency between two variables (X and Y) when the relationship is nonlinear but monotonic. That is, it assesses how well the relationship between two variables can be described with an either linear or nonlinear monotonic relationship. The Spearman's technique requires ranked arrangement of the variables based on their values (e.g. from low to high). Equation 3 measures the statistical dependency between two ranked variables:

$$rho = \frac{\sum_{i=1}^{n}(X_i - \overline{X}) \cdot (Y_i - \overline{Y})}{\sqrt{\sum_{i=1}^{n}(X_i - \overline{X})^2 \cdot \sum_{i=1}^{n}(Y_i - \overline{Y})^2}} \qquad \text{Equation 3}$$

where Y is the ranked output variable and X is the ranked input parameter. The sign of the Spearman correlation indicates the direction of the association between X and Y and a higher absolute value means a stronger correlation.

In general, the technique provides values between -1 and +1, where +1 is perfect the positive correlation and -1 is the perfect negative correlation. If Y tends to increase or decrease when X increases, the coefficients are positive or negative, respectively. A perfect Spearman correlation of +1 or -1 occurs when each of the X variables is a perfect monotonic function of Y. In addition, zero value indicates that there is no tendency for Y to either increase or decrease when X changes.

Here the Spearman's rank correlation coefficients technique was used to quantify the impact of individual input parameters on the desired output variable (PI). Fig 3 shows the Spearman correlation coefficients between the pertinent parameters and PI values for the case with K_m=0.01 mD at different times during the 20-year production period. The results illustrate that N_f is the most important parameter affecting PI during the entire well lifetime. The X_f effect decreases from 0.54 to 0.28, almost half of its initial value, over the entire 20-year production period while the impact of fracture spacing increases from zero at the early time of 1 day of production to over 0.43 after approximately 1 year of the production reaching to 0.47 at boundary dominated flow period. The graph also shows that the fracture permeability and width impacts are small. In other words, the results indicate that at PSS conditions increasing the fracture width and permeability do not result in a significant increase in PI of these low permeability formations while changing fracture half-length, spacing and numbers influences PI greatly.

4. Symbolic Regression

The model (equation) selection is the task of selecting the most efficient (mathematical) model from a set of potential models to provide a predictive tool for a given input-output data.

Generally, as the number of the effective parameters increases, the equation becomes more complex particularly if only data driven techniques, relating the output to a large number of possible input variables, is adopted. In addition, traditional regression methods optimise coefficients of an equation with a specific form, for example, power law equation, such that the function is developed with a small percentage of fitting error and predicts the output reasonably satisfactory.

In many areas, applying such approaches are not desirable. It is often preferable that the sought models are descriptive of the relations between response and variables, capable of satisfactorily predicting new sample responses while honouring scientific explanations and expected trends. For such cases, a new type of regression techniques such as the symbolic regression should be applied.

The Symbolic regression method, unlike traditional regression methods, searches the space of mathematical expressions to deliver the model that best fits a given dataset, both in terms of accuracy and simplicity. The Symbolic regression technique uses Genetic programming to seek both the form of equations and the coefficients simultaneously by combining different mathematical building blocks such as mathematical operators, constants, analytic functions and state variables. Genetic programming, which is an artificial intelligence method, is encoded as a set of genes that are modified then using an evolutionary algorithm whilst recombining previous equations. The technique provides a set of equations that fit data properly and ranks them based on common fitness and complexity measures, so one could choose the most appropriate equation.

For the case of MFHWs considered here, if the traditional regression methods for relating input parameters ($N_f, S_f, W_f, X_f, K_f, K_m, r_w, r_e, H, \mu, B$) and output parameter (PI) are used, it would lead to developing a complex and uninterpretable model. Hence, we propose an expression that relates MFHWs-PI ($PI_{n,s}$) to PI of the horizontal well with a single fracture (PI_{1f}), the number of fractures (N_f) and dimensionless fracture spacing parameters (S_x) as follows:

$$PI_{n,s} = f\left(N_f, S_x, PI_{1f}\right) \qquad \text{Equation 4}$$

$$S_x = \frac{S_f}{X_e} \qquad \text{Equation 5}$$

$$PI_{1f} = f(W_f, X_f, K_f, K_m, r_w, r_e, H, \mu, B) \qquad \text{Equation 6}$$

where PI_{1f} is productivity index of the well with the same specifications but including only one fracture, X_e is the drainage half-length in the X direction and $PI_{n,s}$ is the total productivity index of MFHWs. Introducing these variables reduce the complexity of the equation as for instance, PI_{1f} accommodates the impact of all single fracture properties into one parameter. The relationship between PI_{1f} and the relevant pertinent parameters is described later in section 5. Then we applied symbolic regression to develop a general, reliable and simple equation for prediction purposes which benefits from limited, appropriate dimensionless numbers with excellent values of fitting indices.

4.1 Development and Validation of PI of MFHWs

2000 data points (PI values of various MFHWs designs), sampled by Latin Hypercube sampling, were split into a training data set and a validation data set. The training set was used to generate and optimize the solution, and the validation set was used to test how well the model predicts the new data. Almost 80% of the total number of the generated data (1600 data points) were randomly selected to be used in the training part of the Equation. The rest of data (20%) were used to validate the reliability of the developed equation. It should be noted that at this stage, we used PI_{1f} values obtained from the reservoir simulator for various configurations.

A commercial software was used to apply symbolic regression technique on the training data for delivering several equations which correlate the three input parameters (N_f, S_x, PI_{1f}) and predict the PI values of MFHWs $(PI_{n,s})$ with minimum errors possible. Then, prediction capability of the delivered equations was evaluated by comparing their outputs with data points in the validation data set. Following this exercise, Equation 7 is chosen as the simplest, the most reliable and explanatory equation among all the suggested equations to calculate PI of MFHWs in tight reservoirs.

$$PI_{n,s} = PI_{1f} + 3.5 N_f S_x PI_{1f} \log N_f \qquad \text{Equation 7}$$

To validate the equation developed for calculating the productivity of MFHWs, results of Equation 6 was compared with the reservoir simulation outputs for a wide range of pertinent parameters. Fig 4 and Fig 5 plot the predicted values by the proposed equation versus the simulation model outputs for the training and testing data sets, respectively.

In addition to the graphical demonstration, two common numerical measures for performance evaluation: Root Mean Square Error (RMSE) and squared correlation coefficient (R^2) were used. RMSE is a frequently used measure of the difference between values predicted by a model and the values observed from the environment that is being modelled. RMSE of a model with respect to the predicted variable X_{pred} is defined as follows:

$$RMSE = \sqrt{\frac{\sum_{i=1}^{n}(X_{obs,i} - X_{pred,i})^2}{n}} \qquad \text{Equation 8}$$

where X_{obs} is the observed value (by the reservoir model) and X_{pred} is the predicted value, calculated using Equation 7. R^2 defines the strength and direction of the linear relationship between the observed and predicted outputs. R^2 and RMSE of 0.983 and 0.174, achieved for the training data set, (Table 3), confirm the good fitness of the equation to the training data. Then, the testing data set was used to validate the reliability of the proposed equation for data not used for its development. The obtained R^2 and RMSE of 0.980 and 0.21 illustrate the good prediction capability of the equation, (Table 3).

Provided the value of each parameter is within the range stated, the equation is capable of evaluating the performance of various MFHW design and therefore determining the optimum design.

Now, to use Equation 7, more efficiently, an equation is required to calculate PI_{1f}, i.e. the performance of a horizontal well with single fracture with the same characteristics as MFHWs.

5. Single Fractured Horizontal Well Performance

5.1 Single Fractured Horizontal Well Versus Fractured Vertical Well

To calculate the performance of a horizontal well with a single fracture (SFHW), i.e. PI_{1f}, we turn our attention to a fractured vertical well case. For a fractured vertical well (FVW), the fracture is in lateral contact with the wellbore so, in the fracture, there is only linear flow to the wellbore (Fig 6). However, as shown in Fig 7, the fluid flow pattern in the fracture of a hydraulically fractured horizontal well is comprised of linear flow (far from the wellbore) and radial flow (near wellbore).

Fig 8 shows pressure profiles of two cases with one either finite (15 mD.ft) or infinite (3000 mD.ft) conductivity fracture having X_f= 650 ft induced on a horizontal well in a reservoir with the permeability of 0.1 mD producing under the pseudo steady state flow regime. This Figure illustrates pressure profiles from fracture tip (Point. 12) toward the wellbore (Point. 1). It shows that the pressure loss within fracture as the fluid travels from point 12 (fracture tip) to 1 (wellbore) is almost 4 psi for the infinite fracture, and 344 psi for the finite fracture one. It is also noted that 37% and 19% of the total pressure loss for the finite and infinite fractures occurred within 25 ft of the fractures near wellbore (referred to point 1-5 in Fig 8) due to radial flow near the wellbore. This additional radial flow, compared to full linear flow for the vertical well, can be treated as a convergence skin (S_c) that provides an extra pressure drop as described in Section 5.2.

5.2 PI of Horizontal Wells with a Single Fracture

The Equivalent open-hole concept is usually used to model fluid flow from the reservoir to the fracture and then to the wellbore. The Equivalent open-hole modelling is a concept in which complex wellbore geometries are transferred into an equivalent open-hole vertical well using a skin factor or effective wellbore radius. In the case of Darcy flow, this skin should represent the difference in geometries between complex wellbore geometry and its equivalent open-hole vertical well. This skin is called “geometric skin” since it represents wellbore geometry effects. In other words, using this skin (or effective wellbore radius) we can define an equivalent open-hole vertical well that should give the same performance as that of a complex wellbore geometry.

Equation 9 is usually used to calculate the well productivity for single-phase flow of a slightly compressible fluid around vertical wells:

$$q_{FVW} = \frac{2\pi kh\Delta P}{\mu\left[ln\left(\frac{r_e}{r_w}\right) + s_t - c\right]} \quad \text{Equation 9}$$

Where c is 0 for steady state flow when P is based on the difference between the wellbore and external pressure and is 0.5 if P is based on the average pressure. In the case of pseudo-steady state flow, c is 0.75, when P is based on the average pressure and is 0.5 if P is based on the external pressure. S_t is the total skin, which includes the damage skin (S_d), geometry skin (S_{gf}), and flow skin (S_f) as shown below,

$$S_t = S_d + S_{\mathrm{gf}} + S_f \qquad \text{Equation 10}$$

For Darcy flow, S_f is zero. Here the damage skin was assumed zero as well. Accordingly, the productivity of fractured vertical wells (FVWs) can be expressed in term of the productivity of vertical well with a fracture geometric skin factor (S_{gf}) also known as Pseudo-Fracture skin, as shown below.

$$q_{FVW} = \frac{2\pi kh\Delta P}{\mu\left[ln\left(\frac{r_e}{r_w + x_f}\right) + s_{\mathrm{g}f} - c\right]} \qquad \text{Equation 11}$$

The wellbore radius r_w can be neglected compared to the fracture half-length (X_f), hence Equation 11 can be written as:

$$q_{FVW} = \frac{2\pi kh\Delta P}{\mu\left[ln\left(\frac{r_e}{x_f}\right) + s_{\mathrm{gf}} - c\right]} \qquad \text{Equation 12}$$

where r_e is the exterior radius of the reservoir model, which for a rectangular drainage area, A can be calculated as follows:

$$r_e = \sqrt{\frac{A}{\pi}} \qquad \text{Equation 13}$$

Geometric skin formulations (S_{gf}), which depends on C_{fd} and I_y, for pseudo-steady state conditions can be calculated by Equation 14 [19].

$$S_{\mathrm{g}f} = \ln(\varepsilon_{PSS} + (\frac{\pi}{\mathrm{g}_{\lambda}.C_{fd}})) \qquad \text{Equation 14}$$

where, g_λ is a geometrical parameter related to the drainage area shape and it is a function of dimensionless fracture conductivity (C_{fd}), penetration ratio (I_y) and reservoir aspect ratio ($\lambda=Y_e/X_e$) as below:

$$g_\lambda = \frac{2e^{-2.C_{fd}.I_y^2}}{1+\frac{1}{\lambda}} + \frac{2.\lambda.(1-e^{-2.C_{fd}.I_y^2})}{1+\frac{1}{\lambda}} \qquad \text{Equation 15}$$

The penetration ratio (I_y) term, defined as the ratio of fracture half-length to drainage half-length in the Y direction, is used to present the geometrical parameter (relative size) of the fracture as shown in Equation 16.

$$I_y = \frac{X_f}{Y_e} \qquad \text{Equation 16}$$

The term (ε_{pss}) is the ratio of the length of fracture to the effective wellbore radius for infinite conductivity fracture under PSS conditions as follows:

$$\varepsilon = \frac{X_f}{r'_w|_{C_{fd\to\infty}}} \qquad \text{Equation 17}$$

Raghavan and Hadinoto [21] showed that for a penetration ratio of less than 0.2 ($I_y \leq 0.2$), the effective wellbore radius of an infinite conductivity fracture is equal to half of the fracture half-length i.e. ε_{pss}=2. Mahdiyar et al. [22] presented two formula for calculating ε at steady state and pseudo steady state flow conditions when I_y>0.2. The following equation was proposed to calculate (ε_{pss}) for fractures with I_y>0.2 in the pseudo-steady state condition:

$$\varepsilon_{pss} = 2\ln\left(e + \frac{0.64}{(\frac{2}{\sqrt{\pi}I_y} - 0.746)^{1.283}}\right) \qquad \text{Equation 18}$$

Fig 9 shows predictions of the reservoir simulation model for both vertical and single fractured horizontal wells for different fractured well cases described in Table 4 (with K_m=0.1 mD, W_f=4 mm, K_f= 1, 10, 100 and 200 D and X_f=110, 330 and 650 ft). It also shows the results of the PI model that is obtained by integrating (Equation 12-Equation 18) for these cases. The data confirm the good agreement between the results of the analytical model and the reservoir simulation outputs for FVWs. This Figure also illustrates the difference between the performances of the horizontal and its corresponding vertical well.

As noted in the Figure, for SFHW and compared to FVW, an additional term, accounting for the extra pressure drop due to radial flow around the wellbore, is required to be included in the FVWs equation to make it applicable to SFHWs. This additional pressure drop, as discussed above, is due to the difference in flow within the fracture to the wellbore between FVW and SFHW geometries. Accordingly, below an analytical equation is used for the calculation of this convergence skin.

The pressure drop (ΔP_R) due to radial flow in the fracture with an outer radius of half-reservoir height (h/2) and a width of W_f can be calculated by:

$$\Delta P_R = \frac{q\mu}{2\pi K_f W_f} ln \frac{h}{2r_w} \qquad \text{Equation 19}$$

The pressure drop due to the linear flow ΔP_L at near wellbore within the fracture with the length of h/2, the width of W_f, and length of h can be written as:

$$\Delta P_L = \frac{(q/2)\mu(\frac{h}{2})}{K_f W_f h} \qquad \text{Equation 20}$$

Subtracting Equation 19 from Equation 20 gives ΔP_s that is the pressure drop due to the flow convergence,

$$\Delta P_s = \Delta P_R - \Delta P_L = \frac{q\mu}{2\pi K_m h}\left[\frac{K_m h}{K_f W_f}\left(\ln\frac{h}{2r_w} - \frac{\pi}{2}\right)\right] \qquad \text{Equation 21}$$

which can be converted to convergence skin as follows [7]:

$$S_c = \frac{K_m h}{K_f W_f}\left(\ln\frac{h}{2r_w} - \frac{\pi}{2}\right) \qquad \text{Equation 22}$$

This Equation, which assumes no direct flow from the reservoir to the wellbore, illustrates that the convergence skin value depends on many parameters such as matrix permeability (K_m), reservoir thickness (h) and fracture permeability (K_f), e.g. if K_mh product is large or K_f is small, then S_c is large. Table 5 shows PI values of different cases with reservoir thickness of either 200 or 300 ft. This Table also includes the relative PI values that represent PI of the case under study to the corresponding base case with (h=100 ft). These data show that relative PI does not increase linearly with reservoir thickness, as it would do for a vertical well mainly due to the presence of convergence skin in the horizontal well case. It should be noted that in this study, a constant fracture conductivity along the fracture was assumed. In the case of having a different conductivity at the near wellbore region, the corresponding values of the near wellbore parameters should be used for calculation of S_c in Equation 22.

In summary, the productivity of SFHWs for a slightly compressible fluid at PSS conditions in field units can be calculated using the following equation:

$$PI_{1f} = \frac{kh}{141.2\ \mu B\left[ln\left(\frac{r_e}{x_f}\right) + s_{\mathrm{g}f} + s_c - 0.75\right]} \qquad \text{Equation 23}$$

where μ and B are the viscosity and formation volume factor respectively. The S_{gf} and S_c are calculated by Equation 14 and Equation 22, respectively.

5.2.1 Validation of PI Model of Horizontal Well with One Vertical Fracture

To validate the equation developed for calculating PI of SFHWs, Equation 23, the predicted values by this equation were compared with the reservoir simulation outputs for 360 configurations of SFHWs with Iy<0.2, as shown in Fig 10, while the other parameters varied as per data listed in Table 2. The predicted results of the equation, compared with the reservoir simulation results in Fig 11, are promising as confirmed by the statistical measures of RMSE of 0.013 (Table 3) and R^2 of 0.99.

In addition, new data sets with I_y>0.2 when (X_f= 880, 1100, 1320, 1540, 1760, 1980 and 2200 ft) were modelled to further investigate the validity of its predictions. Fig 12 confirms the accuracy of the developed equation for the configurations tested with I_y>0.2, where acceptable RMSE of 0.059 and R^2 of 0.99 are noted, (Table 3).

Summary and Conclusion

The following can be pointed out about this study:

1. A new approach was followed to develop a new productivity index model estimating the performance of multiple fractured horizontal wells with complex 3D flow features in tight reservoirs. That is, the productivity index of multiple fractured horizontal wells (MFHWs-PI) was related to productivity index (PI) of the horizontal well with a single fracture (SFHW) and to the number of fractures and dimensionless fracture spacing parameter by applying the symbolic regression technique.
2. Symbolic regression along with the Latin Hyperbolic sampling method was used to deliver Equation 7 capturing the multiple fractured horizontal wells flow performance including the fracture interference.
3. The proposed equation is general, reliable and simple for prediction purposes in tight reservoirs because it benefits from limited, appropriate dimensionless numbers with excellent fitting indices values.
4. In a sensitivity study, it was shown that the impacts of the pertinent parameters on productivity index vary during the whole production period depending on the governing flow regimes. Moreover, the results indicated that at pseudo steady state conditions increasing the fracture width and permeability do not result in a significant increase in PI for the low permeability formations considered while changing fracture half-length, spacing and numbers influences productivity index greatly at pseudo steady state condition.

5. This study expands our understanding of flow behaviour in tight reservoirs and provides an invaluable engineering tool that can facilitate simulation of flow around multiple fractured horizontal wells and quickly predict the corresponding well performance.

Acknowledgments

The above study was conducted as a part of the Unconventional Gas and Gas-condensate Recovery Project at Heriot-Watt University. This research project is sponsored by Daikin, DEA, Dong Energy, Ecopetrol/Equion, ExxonMobil, GDF, INPEX, JX-Nippon, Petrobras, Saudi-Aramco and TOTAL, whose contributions are gratefully acknowledged. The authors also thank Schlumberger Information Solutions, Nutonian and MathWorks for access to their software.

Unit Conversion:

ft = 0.3048 Meter
inch= 0.0254 Meter
psi= 0.0689476 Bar
psi= 6894.76 Pascal
$T_{(°C)} = (T_{(°F)} - 32) \times 5/9$
Darcy = 9.86923e-13 m^2

Nomenclature:

B	Formation volume factor	RMSE	Root mean square error
C_{fd}	Dimensionless fracture conductivity	r_e	Drainage radius
FVWs	Fractured vertical wells	r_w	Wellbore radius
h	Formation thickness	R^2	Squared correlation coefficient
I_y	Penetration ratio	S_c	Convergence skin
K_m	Matrix permeability	S_f	Fracture spacing
K_f	Fracture permeability	S_{gf}	Flow geometry skin
MFHWs	Multiple fractured horizontal wells	SFHWs	Single fractured horizontal wells
PI	Productivity index	X_e	Drainage half-length in X direction
P_{wf}	Flowing Bottom-hole pressure	Y_e	Drainage half-length in Y direction
$\bar{P}_r$	Reservoir pressure	μ	Viscosity of the fluid
Q	Gas production rate		

References

[1] J.E. Brown, M.J. Economides, An Analysis of Horizontally Fractured Horizontal Wells, in, Society of Petroleum Engineers, 1992.

[2] R. Raghavan, S.D. Joshi, Productivity of Multiple Drainholes or Fractured Horizontal Wells, SPE Formation Evaluation, 8 (1993).

[3] M.-y. Xu, Q.-q. Ran, G.-z. Shen, N. Li, A study on unsteady seepage field of fractured horizontal well in tight gas reservoir, Journal of the Energy Institute.

[4] L. Tian, C. Xiao, M. Liu, D. Gu, G. Song, H. Cao, X. Li, Well testing model for multi-fractured horizontal well for shale gas reservoirs with consideration of dual diffusion in matrix, Journal of Natural Gas Science and Engineering, 21 (2014) 283-295.

[5] F.M. Giger, Horizontal Wells Production Techniques in Heterogeneous Reservoirs, in, Society of Petroleum Engineers, 1985.

[6] G. Guo, R.D. Evans, Inflow Performance and Production Forecasting of Horizontal Wells With Multiple Hydraulic Fractures in Low-Permeability Gas Reservoirs, in: Society of Petroleum Engineers, Society of Petroleum Engineers, 1993.

[7] H. Mukherjee, M.J. Economides, A Parametric Comparison of Horizontal and Vertical Well Performance, SPE Formation Evaluation, 6 (1991) 209 - 216.

[8] S.D. Joshi, Augmentation of Well Productivity With Slant and Horizontal Wells (includes associated papers 24547 and 25308), Journal of Petroleum Technology, 40 (1988) 729-739.

[9] M. Prats, Effect of Vertical Fractures on Reservoir Behavior-Incompressible Fluid Case, Society of Petroleum Engineers Journal, 1 (1961) 105-118.

[10] B. Guo, D.S. Schechter, A Simple And Rigorous IPR Equation For Vertical And Horizontal Wells Intersecting Long Fractures, J Can Petrol Technol, 38 (1999).

[11] F. Kuppe, A. Settari, A practical method for theoretically determining the productivity of multi-fractured horizontal wells, J Can Petrol Technol, 37 (1998) 68-81.

[12] J. Guo, F. Zeng, J. Zhao, Y. Xu, A New Model to Predict Fractured Horizontal Well Production, in, Petroleum Society of Canada, 2006.

[13] S. Amini, P.P. Valkó, Using Distributed Volumetric Sources To Predict Production From Multiple-Fractured Horizontal Wells Under Non-Darcy-Flow Conditions, SPE Journal, 15 (2010) 105-115.

[14] J. Lin, D. Zhu, Modeling well performance for fractured horizontal gas wells, Journal of Natural Gas Science and Engineering, 18 (2014) 180-193.

[15] W. Yu, K. Sepehrnoori, An Efficient Reservoir-Simulation Approach To Design and Optimize Unconventional Gas Production, J Can Petrol Technol, 53 (2014).

[16] M.T. Baig, S. Alnuaim, M.H. Rammay, Productivity Increase Estimation for Multi Stage Fracturing in Horizontal Wells for Tight Oil Reservoirs, in: SPE Saudi Arabia Section Annual Technical Symposium and Exhibition, Society of Petroleum Engineers, Al-Khobar, Saudi Arabia, 2015.

[17] M. Jamiolahmady, E. Alajmi, H.R. Nasriani, P. Ghahri, K. Pichestapong, A Thorough Investigation of Clean-up Efficiency of Hydraulic Fractured Wells Using Statistical Approaches, in, Society of Petroleum Engineers, 2014.

[18] M.D. McKay, R.J. Beckman, W.J. Conover, A Comparison of Three Methods for Selecting Values of Input Variables in the Analysis of Output from a Computer Code, Technometrics, 21 (1979) 239-245.

[19] B.R. Meyer, R.H. Jacot, Pseudosteady-State Analysis of Finite Conductivity Vertical Fractures, in: SPE Annual Technical Conference and Exhibition, Society of Petroleum Engineers, Dallas, Texas, 2005.

[20] M. MoradiDowlatabad, M. Jamiolahmady, The lifetime performance prediction of fractured horizontal wells in tight reservoirs, Journal of Natural Gas Science and Engineering,

42 (2017) 142-156.
[21] R. Raghavan, N. Hadinoto, Analysis of Pressure Data for Fractured Wells: The Constant-Pressure Outer Boundary, Society of Petroleum Engineers Journal, 18 (1978) 130-150.
[22] H. Mahdiyar, M. Jamiolahmady, M. Sohrabi, Improved Darcy and non-Darcy flow formulations around hydraulically fractured wells, Journal of Petroleum Science and Engineering, 78 (2011) 149-159.
[23] M. MoradiDowlatabad, M. Jamiolahmady, The Performance Evaluation and Design Optimisation of Multiple Fractured Horizontal Wells in Tight Reservoirs, Journal of Natural Gas Science and Engineering, 46 (2017).

Table 1: Reservoir Parameters

Parameter	Empirical		SI	
	Value	Unit	Value	Unit
Reservoir pressure	7500	psi	5.1711e+7	N/m^2
Reservoir temperature	200	ºF	93	ºC
Reservoir porosity	0.15		0.15	
Reservoir depth	14800	ft	4511	m
Well Diameter	4.5	inch	0.1143	m

Table 2: Parameters and their variation ranges

Parameter	Min	Max	Distribution
Matrix permeability (K_m)	0.001 mD (9.87e-16 m^2)	0.1 mD (9.87e-14 m^2)	Uniform
Number of Fractures (N_f)	1	15	Uniform
Fracture Spacing (S_f)	80 ft (24.38 m)	650 ft (198.10 m)	Uniform
Fracture Half-Length (X_f)	100 ft (30.48 m)	1020 ft (310.90 m)	Uniform
Fracture Width (W_f)	0.002 m	0.008 m	Uniform
Fracture Permeability (K_f)	10 D (9.87e-12 m^2)	200 D (1.974e-10 m^2)	Uniform

Table 3: The RMSE and R^2 indices for the developed equations

Equations			RMSE	R^2
1	MFHWs (Training set)		0.174	0.983
2	MFHWs (Testing set)		0.210	0.980
3	SFHWs	I_y< 0.2	0.013	0.99
		I_y> 0.2	0.059	0.99

Table 4: The specification of the cases used to compare PI of FVWs with PI of SFHWs as shown in Fig 9.

No.	X_f (ft)	K_f (D)	K_m (mD)
1	110	1	0.1
2	110	10	0.1
3	110	100	0.1
4	110	200	0.1
5	330	1	0.1
6	330	10	0.1
7	330	100	0.1
8	330	200	0.1
9	650	1	0.1
10	650	10	0.1
11	650	100	0.1
12	650	200	0.1

Table 5: Relative PI changes due to formation height changes for some MFHWs.

No	X_f (ft)	K_f (D)	K_m (mD)	C_{fd}	PI (MScf/Day.psi)			Relative PI	
					H100	H200	H300	H200	H300
1	110	1	0.005	27.3	0.054	0.103	0.146	1.90	2.70
2	110	1	0.1	1.4	0.536	0.724	0.806	1.35	1.50
3	110	10	0.005	272.7	0.057	0.113	0.169	1.99	2.97
4	110	10	0.1	13.6	0.960	1.756	2.400	1.83	2.50
5	110	10	0.005	2727.3	0.057	0.114	0.172	2.00	3.00
6	110	100	0.1	136.4	1.051	2.082	3.078	1.98	2.93
7	110	200	0.005	5454.5	0.057	0.114	0.172	2.00	3.00
8	110	200	0.1	272.7	1.057	2.104	3.128	1.99	2.96
9	330	1	0.005	9.1	0.075	0.140	0.196	1.86	2.60
10	330	1	0.1	0.5	0.562	0.748	0.826	1.33	1.47
11	330	10	0.005	90.9	0.084	0.166	0.247	1.99	2.95
12	330	10	0.1	4.5	1.245	2.221	2.970	1.78	2.39
13	330	10	0.005	909.1	0.085	0.170	0.254	2.00	3.00
14	330	100	0.1	45.5	1.488	2.937	4.316	1.97	2.90
15	330	200	0.005	1818.2	0.085	0.170	0.255	2.00	3.00
16	330	200	0.1	90.9	1.506	2.993	4.432	1.99	2.94

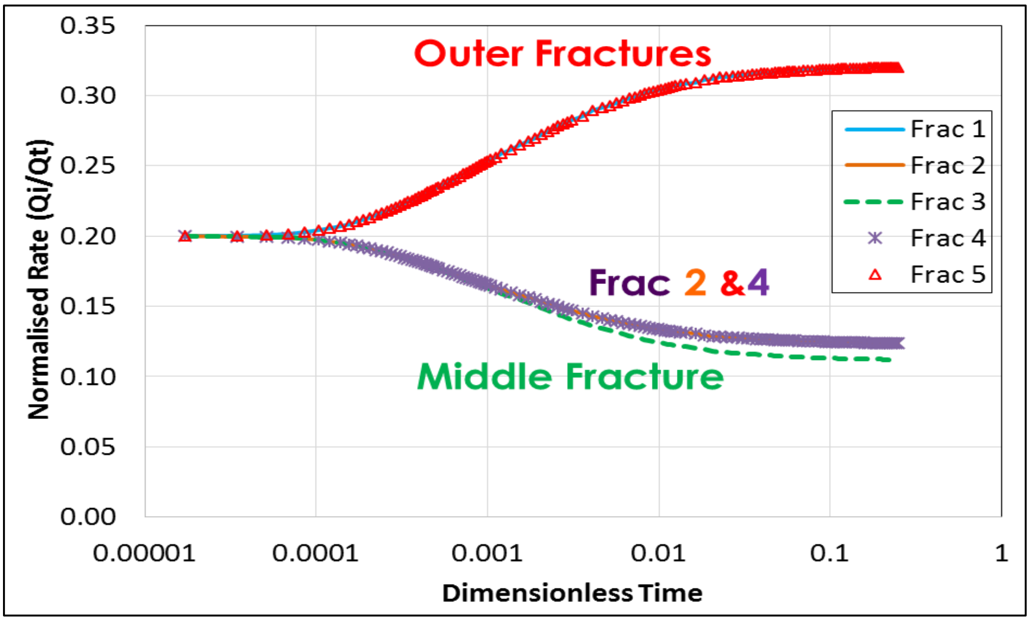

Fig 1: The normalized rate of each fracture versus dimensionless time for the model with N_f=5 in Fig 2.

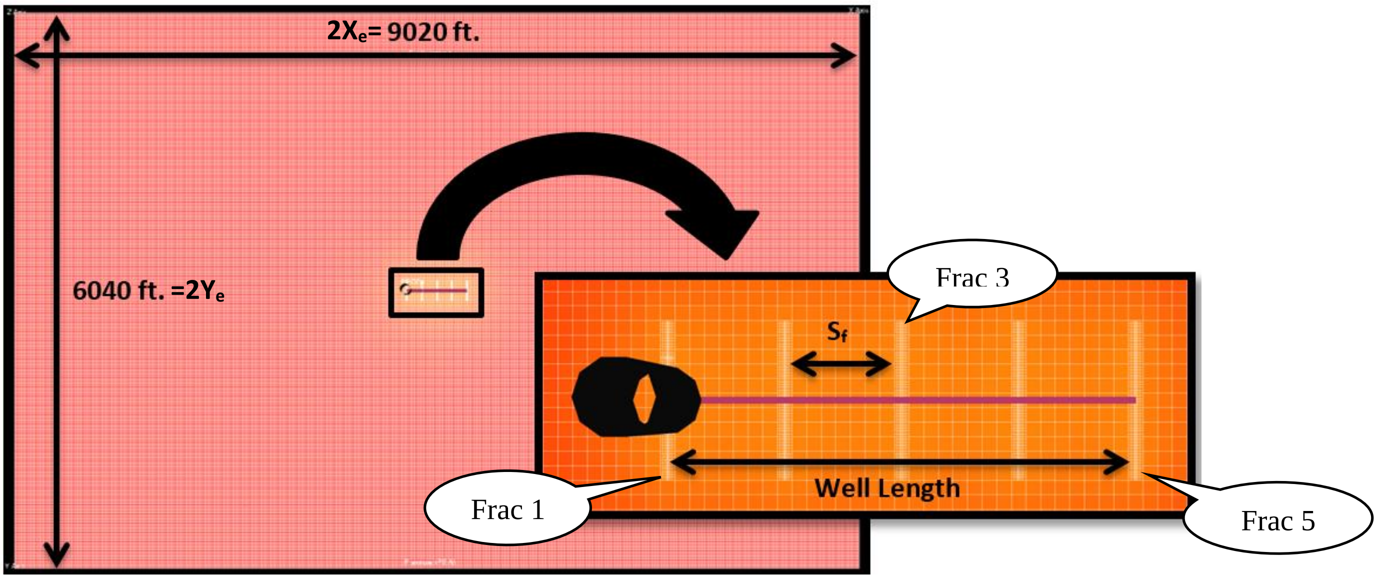

Fig 2: A schematic diagram of Reservoir and MFHWs.

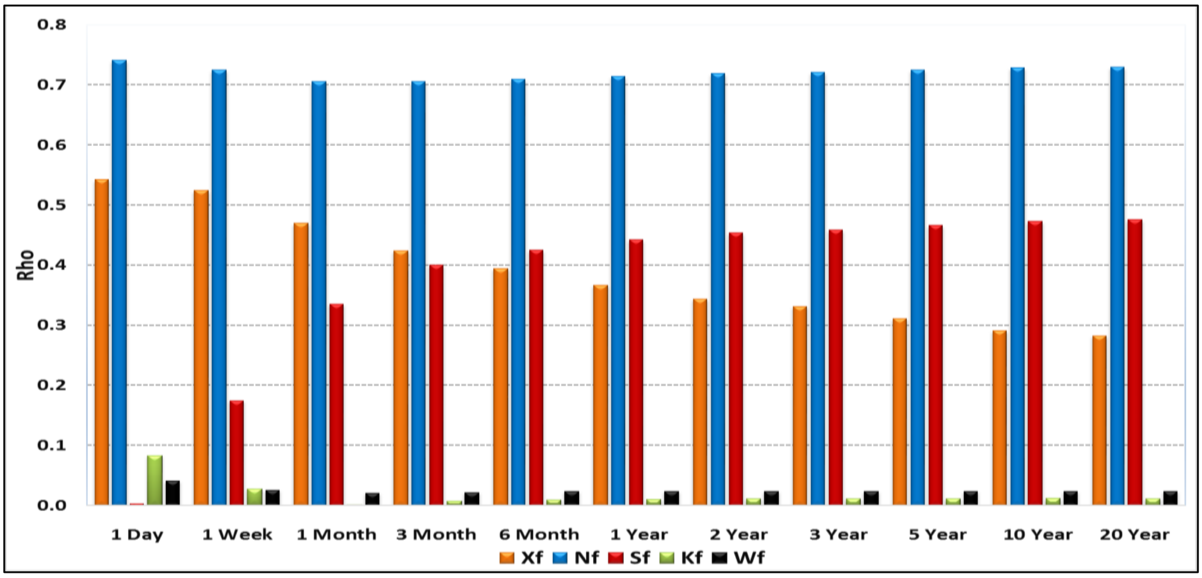

Fig 3: The impact of five pertinent parameters on PI values over the 20-year well lifetime (K_m=0.01 mD).

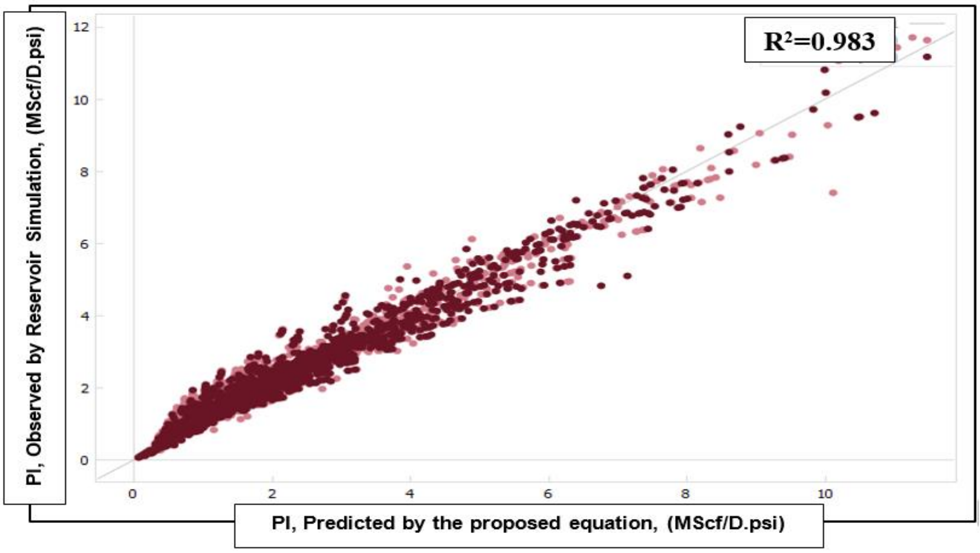

Fig 4: Predicated PI of MFHW by Equation 7 versus simulation results for data used for training of the equation.

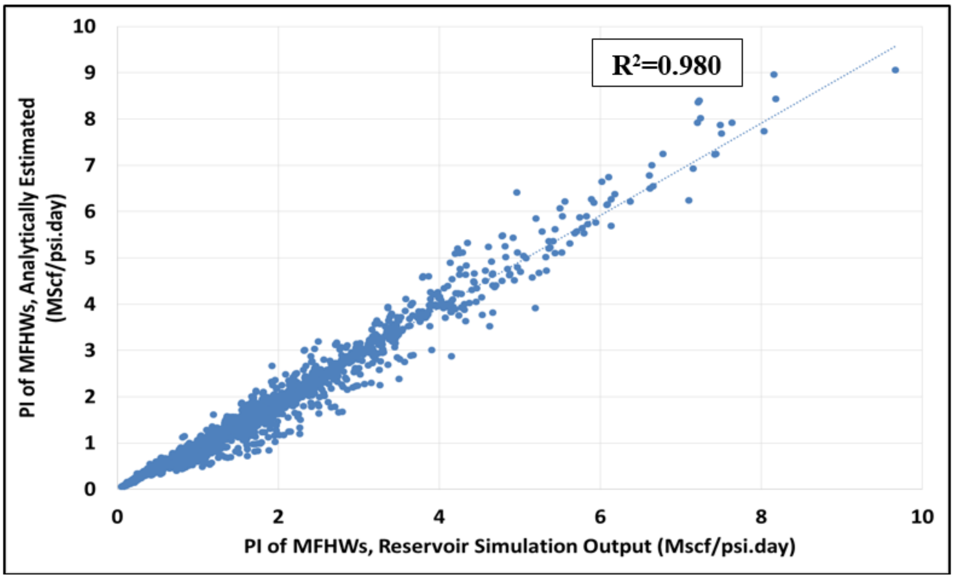

Fig 5: Predicated PI of MFHW by Equation 7 versus simulation results for testing data not used for ~~testing~~ the development of the equation.

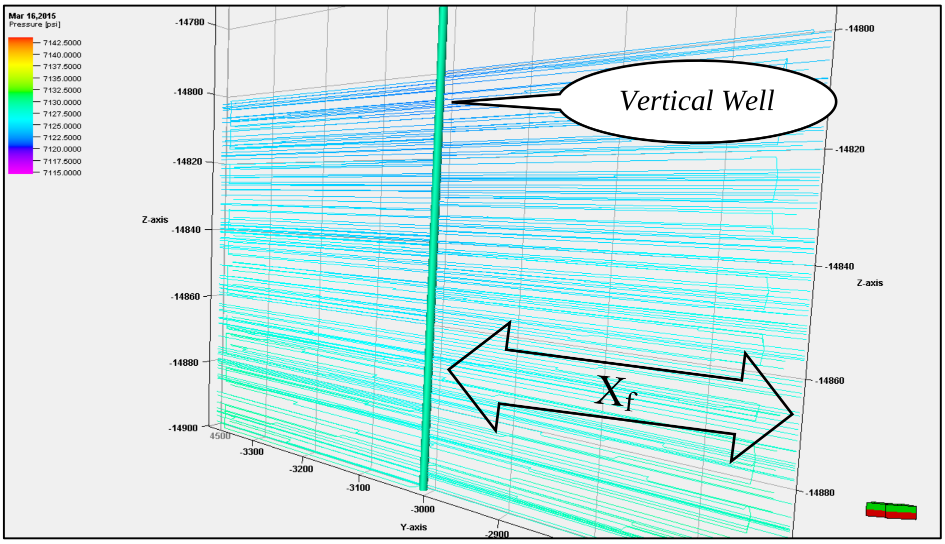

Fig 6: Pressure profile streamlines around a fractured vertical well.

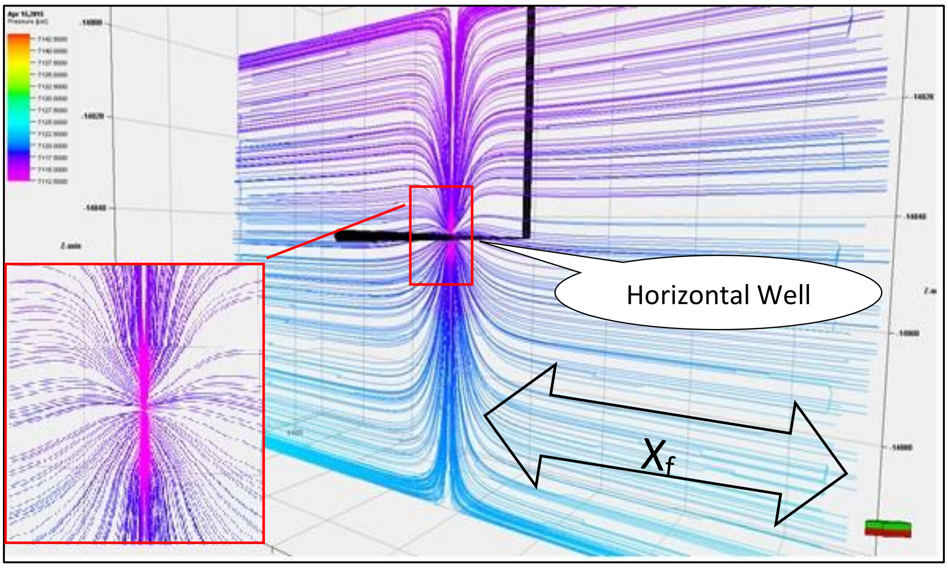

Fig 7: Pressure profile streamlines illustrating convergence due to the radial flow near the wellbore of a single fractured horizontal well.

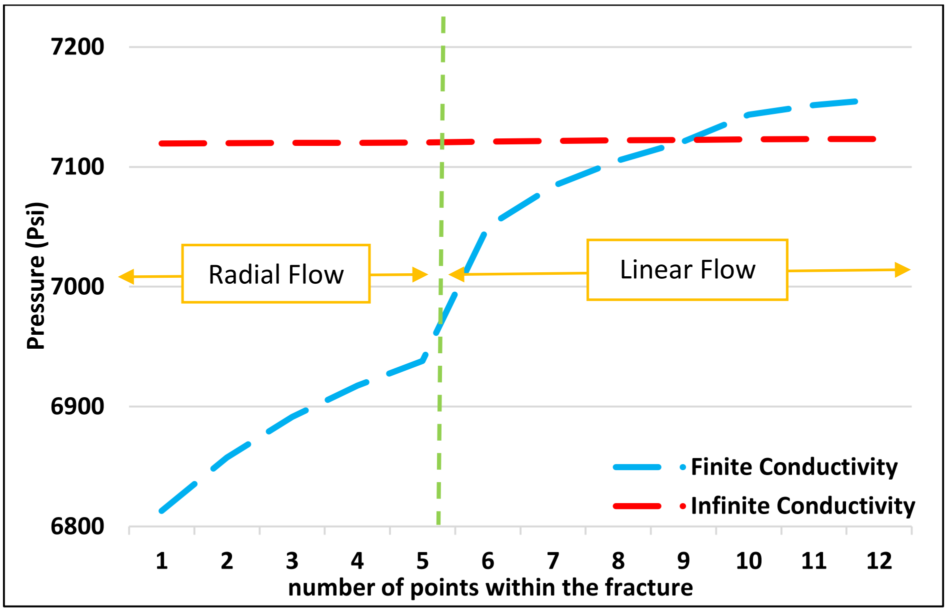

Fig 8: Pressure drop across a fracture with finite and infinite conductivity. (K_m= 0.1 mD, K_f= 1 and 200 D, X_f= 650 ft, W_f=0.015 ft and N_f=1).

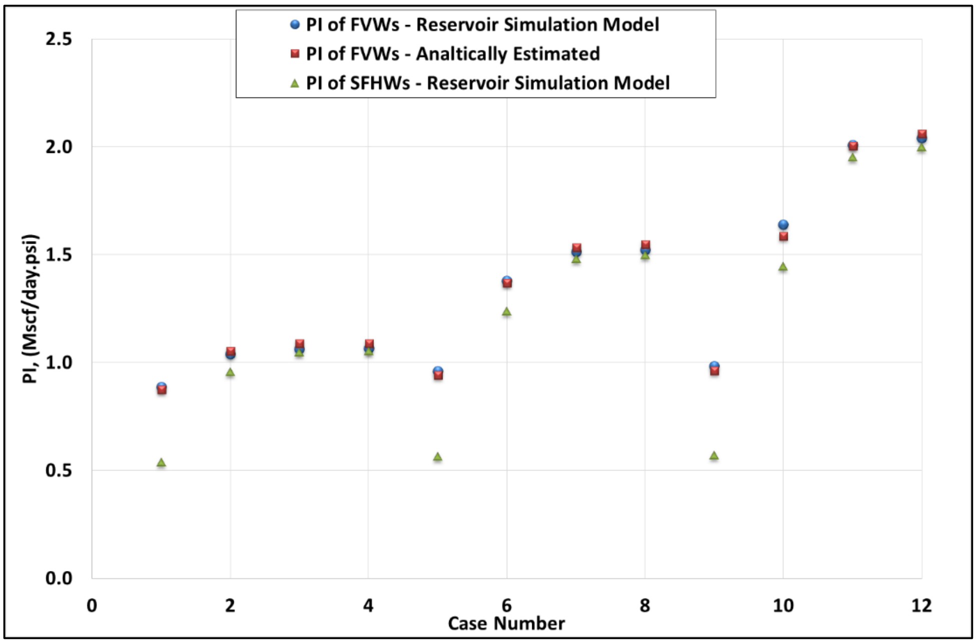

Fig 9: Predicated PI of FVWs versus simulation results for both single-fracture horizontal and vertical wells, (K_m=0.1 mD, W_f=4 mm, K_f= 1, 10, 100 and 200D and X_f=110, 330 and 650 ft, the cases here correspond to those in Table 4).

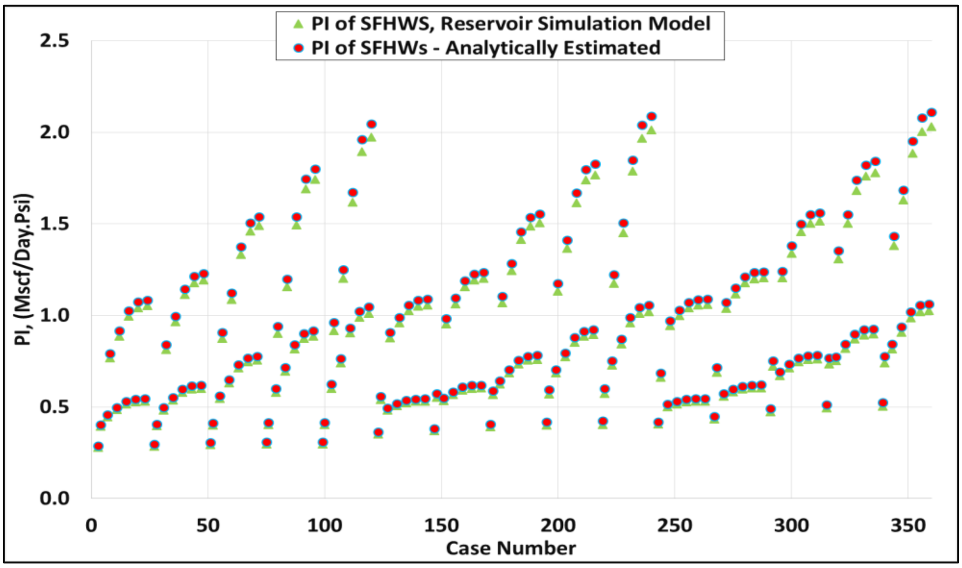

Fig 10: Predicted PI of SFHWs by Equation 23 versus simulation results.

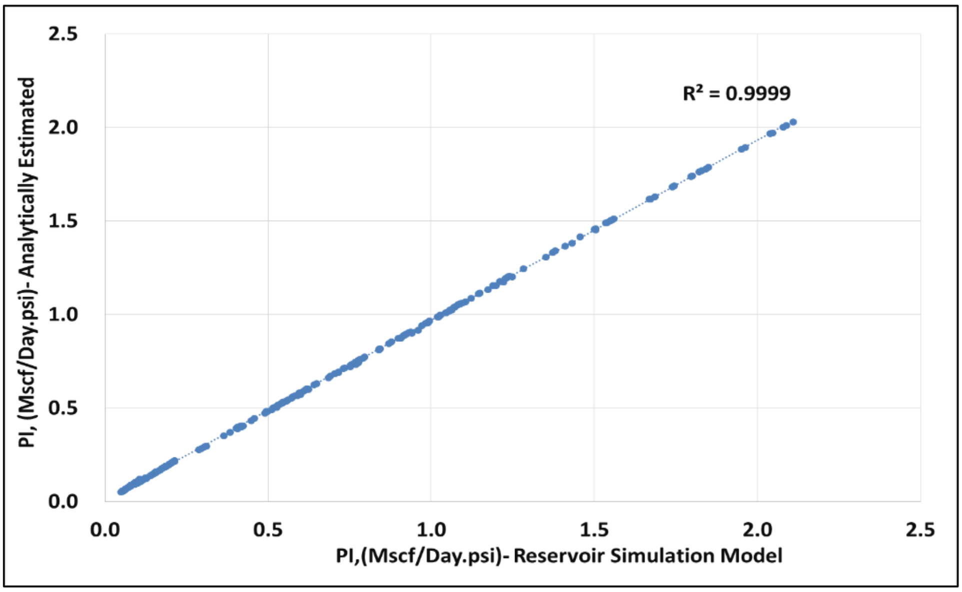

Fig 11: Predicted PI of SFHWs by Equation 23 versus simulation results when $I_y < 0.2$.

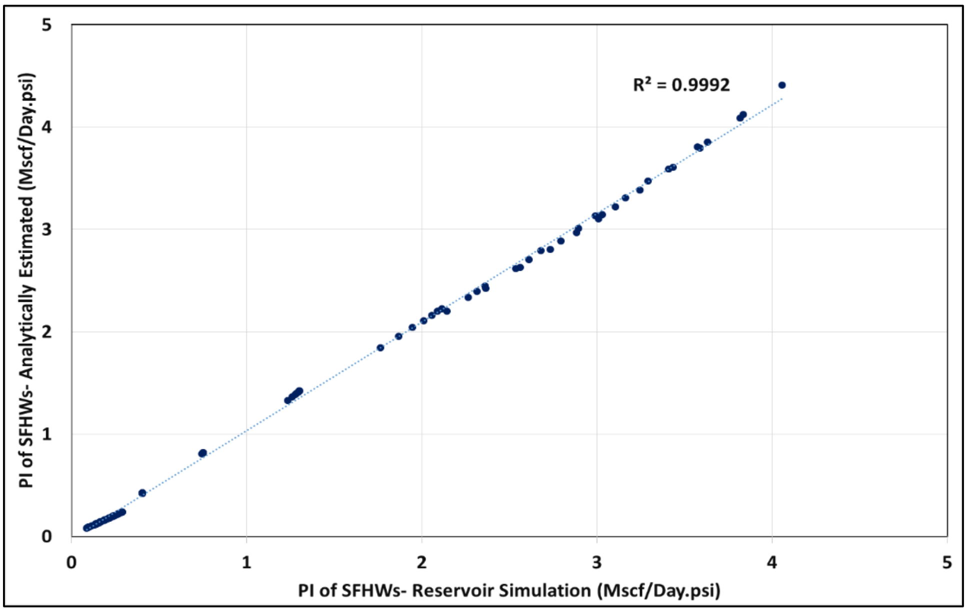

Fig 12: Predicted PI of SFHWs by Equation 23 versus simulation results when I_y>0.2.